TECHNICAL FEASIBILITY ASSESSMENT OF A RECUPERATOR IN REVERSIBLE TRANS-CRITICAL CO2 HEAT PUMP/RANKINE CYCLE: CONSIDERING SCROLL MACHINE OPERATION BOUNDARIES

Bentao Guo[1]*, Aitor Cendoya[2], Vincent Lemort[3]

[1]Thermodynamics Laboratory, University of Liege, 4000 Liege, Belgium

[2]Thermodynamics Laboratory, University of Liege, 4000 Liege, Belgium

[3]Thermodynamics Laboratory, University of Liege, 4000 Liege, Belgium

*Corresponding Author: Bentao.Guo@uliege.be

ABSTRACT

Carnot batteries are getting more attention rapidly, as a potential energy storage technology coupled with variable renewable energy. Trans-critical heat pumps (THP)/Rankine cycles (TRC) using a natural fluid CO_2 perform well with a sensible hot storage of a large temperature spread, and their capital cost can be further reduced in a reversible configuration. This study proposes a reversible THP/TRC based on a reversible scroll machine with hot storage but without cold storage for a small-scale family farm, using the ambient air as the secondary fluid of the evaporator/condenser in THP/TRC, respectively. The study assesses the feasibility of a recuperator in the reversible THP/TRC under optimal and limited operation ranges, taking into account the maximum pressure and temperature of the scroll machine. In optimal operation, the recuperator improves the power-to-power efficiency (*P2P*) up to 28 % (recuperator efficiency is 0.75) and reduces the optimal high pressure of both THP/TRC. In the limited operation, *P2P* is improved by a perfect recuperator up to 57 %, and this value decreases with recuperator efficiency from 1 to 0.25. The extension of the highest scroll pressure contributes to a higher possible hot storage temperature and less affected conditions for basic THP/TRC without a recuperator. The affected conditions in the recuperated THP/TRC are reduced by the higher temperature that the scroll machine can withstand. This work introduces operation boundaries of a reversible scroll machine as constraints in a reversible CO_2 Carnot battery, supplying some reference for its practical system design and operation conditions.

1 INTRODUCTION

With the rapid surge of variable renewable energy (VRE), energy storage becomes more and more crucial, compensating for the VRE's intermittent nature (Caralis *et al.*, 2019). Among various energy storage technologies, pumped thermal energy storage (Carnot battery), where electric energy is stored as thermal energy and later recovered during discharge (Dumont *et al.*, 2020), outstands due to its flexible capacity, long lifetime and minimal dependency on geological sites or resources (Sorknæs *et al.*, 2023). Large-scale trans-critical CO_2 Carnot batteries (TCCB) have been investigated with Technology Readiness Level up to 3 - 4 (Shamsi *et al.*, 2024) and demonstrate better technical and economic performance than other energy storage technologies with sensible hot storage (Zhao *et al.*, 2022), with a highest predicted round-trip-efficiency of 68 % and a lowest capital cost. Shamsi *et al.* (2024) reveal that reversible machines in TCCB should be prototyped to optimize investment costs. Scroll machines have been widely used in vehicle heat pumps (Wang *et al.*, 2023; Zheng *et al.*, 2020) and small-scale ORC (Ayachi *et al.*, 2016a; Dickes *et al.*, 2025; Dumont *et al.*, 2018; Quoilin *et al.*, 2010; Wieland *et al.*, 2023), and they can also act as the dual-function machine in a reversible HP/ORC (Dumont *et al.*, 2021; Guo and Lemort, 2024; Guo *et al.*, 2025; Pezo *et al.*, 2024; Ravindran *et al.*, 2024), but their operation range is limited (Wang *et al.*, 2022).

The recuperator is widely used in trans-critical CO_2 heat pumps (Qin *et al.*, 2021; Song *et al.*, 2022), whose applicability is evaluated deeply by He *et al.* (2023) in water heaters, refrigeration systems, and automotive air-conditioners. However, the low temperature spreads of those applications usually mismatch the requirement of a TCCB (Ayachi *et al.*, 2016b; Baik *et al.*, 2014; Kim *et al.*, 2013). It also functions in trans-critical CO_2 Rankine power cycles (Pan *et al.*, 2016) and even TCCB (Ayachi *et al.*, 2016b; Kim *et al.*, 2013; Zhao *et al.*, 2022) for performance enhancement, and the applicability of the recuperator in a Reversible TCCB (RTCCB) has not been studied yet.

This study aims to investigate the technical feasibility of a recuperator in an RTCCB based on the application to a small-scale family farm. The second section is the case study and proposed system description, and the third section gives the methodology of the work. In the fourth section, based on the condition of the case study, a comparison and discussion of the recuperator applicability is conducted in optimal operation and realistic operation limited by the boundaries of the scroll machine, and a parameter study is given regarding the variation of the recuperator efficiency and machine boundaries.

2 SYSTEM DESCRIPTION

The studied small-scale family farm is in Ben Guerir, Morocco, and its mean temperatures in the day (8:00 – 19:00) and night (19:00 – 8:00) are 23 °C and 17 °C, respectively. The trans-critical HP (THP) is designed to operate during the day using the photovoltaic output, and the trans-critical Rankine cycle (TRC) generates power during the night for irrigation pumps and bulbs. The schematic of the RTCCB is presented in Figure 1, where the HPHX and LPHX correspond to the high-pressure and low-pressure heat exchangers, respectively, and IHX represents the recuperator. A scroll machine is utilized as the reversible compressor/expander. The ambient air during the day is utilized as the heat source of the THP; the ambient air at night acts as the heat sink for the TRC.

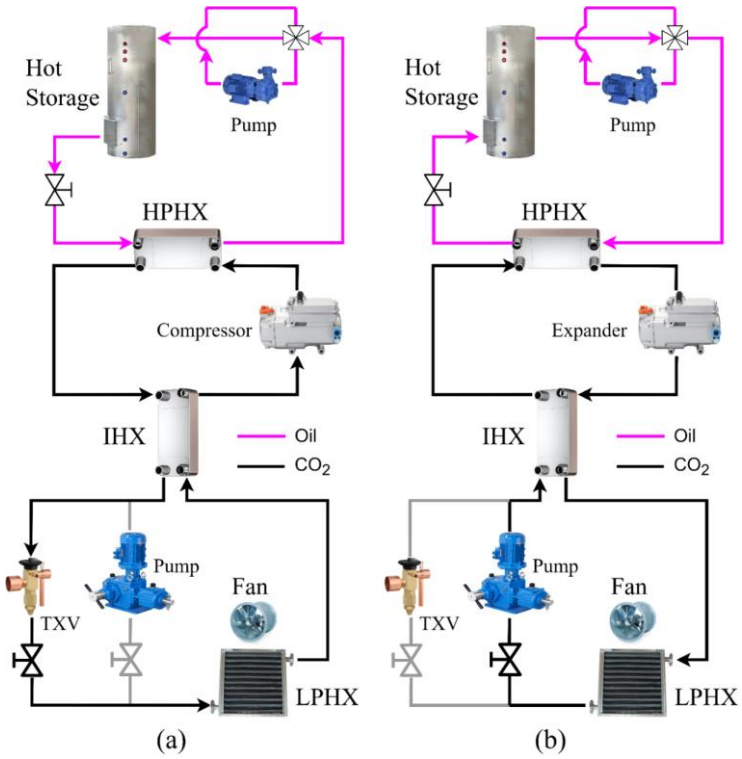

Figure 1: Diagram of RTCCB with a recuperator (a: THP, b: TRC)

In the THP mode, the expanded two-phase CO_2 after the TXV (thermal expansion valve) enters the LPHX (evaporator), absorbing heat from the ambient air, and then passes through the IHX. In the IHX, the CO_2 vapor is heated by high-temperature CO_2 fluid leaving the gas cooler (HPHX), and then

compressed in the compressor, entering the HPHX. The high-temperature CO_2 fluid heats the secondary fluid in the hot storage loop, from the hot storage low temperature ($T_{hot,l}$) to its set high temperature ($T_{hot,h}$). On the other hand, in the TRC mode, after the low-pressure and low-temperature CO_2 is pumped to a high-pressure state by the pump and heated in the IHX by the exhaust high-temperature CO_2 from the expander, it enters the HPHX (gas heater) to get further heated by the secondary fluid in the hot storage loop. Then, the high-pressure and high-temperature supercritical CO_2 is expanded and exhausted to the IHX and further rejects the heat to the ambient air in the LPHX (condenser).

As a benchmark for the adaptability evaluation of the recuperator, the basic system layout is the reversible THP/TRC system in Figure 1 without IHX. Besides, two operational ranges are proposed: the optimal operation (opt.) without scroll machine operation limits (the optimum high pressure of THP/TRC is always reachable), and the limited operation (ltd.) within the machine operation boundaries. In other words, in the limited operation, if the machine pressure or temperature under the optimum pressure is outside the boundary, the system deviates from its optimal condition to work within the boundary (affected condition). As the ambient air is used as the secondary fluid in the LPHX, the performance deviation map under various $T_{hot,l}$ and $T_{hot,h}$ in the hot storage side is given in this study.

3 METHODOLOGY

3.1 System Modelling

All the models are implemented in the MATLAB environment, and a design model for a reversible heat pump/Rankine cycle with fixed pinch points (Guo and Lemort, 2024; Guo *et al.*, 2025) is utilized. The properties of CO_2 are calculated by CoolProp (Bell *et al.*, 2014). The variation step for searching for the optimum high pressure ($P_{cmp,ex}$ in THP, $P_{exp,su}$ in the TRC) is 5 bar. The scroll compressor model is completed by assuming the total compression process is isentropic compression from suction to the adaptive point, firstly, and then a constant-volume process until discharge (Winandy *et al.*, 2002). Similarly, the ideal expansion is also divided into 2 steps: isentropic expansion from the supply to the adaptive point and then constant-volume expansion until the exhaust state (Lemort, 2008). The efficiency of the recuperator is constant and the same in THP/TRC modes, and its heat transfer rate is calculated below (He *et al.*, 2023):

$$\dot{Q}_{IHX} = \eta_{IHX} \times \dot{Q}_{IHX,max} \tag{1}$$

In the THP mode, the maximum heat transfer ($\dot{Q}_{IHX,max,THP}$) is:

$$\dot{Q}_{IHX,max,THP} = \dot{m}_{CO2,THP} \times min\left(h_{gc,ex,CO2} - h_{IHX,h,ex,min,THP}, h_{IHX,l,ex,max,THP} - h_{ev,ex,CO2}\right) \tag{2}$$

$$h_{IHX,h,ex,min,THP} = enthalpy(P = P_{IHX,h,ex,THP}, T = T_{ev,ex,CO2}, CO_2) \tag{3}$$

$$h_{IHX,l,ex,max,THP} = enthalpy(P = P_{IHX,l,ex,THP}, T = T_{gc,ex,CO2}, CO_2) \tag{4}$$

Where subscripts *h* and *l* represent the high-temperature and low-temperature sides of the recuperator, respectively. In the TRC mode, its maximum heat transfer ($\dot{Q}_{IHX,max,TRC}$) is:

$$\dot{Q}_{IHX,max,TRC} = \dot{m}_{CO2,TRC} \times min\left(h_{exp,ex,CO2} - h_{IHX,h,ex,min,TRC}, h_{IHX,l,ex,max,TRC} - h_{pp,ex,CO2}\right) \tag{5}$$

$$h_{IHX,h,ex,min,TRC} = enthalpy(P = P_{IHX,h,ex,TRC}, T = T_{pp,ex,CO2}, CO_2) \tag{6}$$

$$h_{IHX,l,ex,max,TRC} = enthalpy(P = P_{IHX,l,ex,TRC}, T = T_{exp,ex,CO2}, CO_2) \tag{7}$$

The performance indicators of THP/TRC are Coefficient of Performance and cycle thermal efficiency:

$$COP = \frac{\dot{Q}_{gc,CO2,THP}}{\dot{W}_{cmp,CO2,THP} + \dot{W}_{pp,oil,THP} + \dot{W}_{fan,a,THP}} \tag{8}$$

$$\eta_{TRC} = \frac{\dot{W}_{exp,CO2,TRC} - \dot{W}_{pp,CO2,TRC} - \dot{W}_{pp,oil,TRC} - \dot{W}_{fan,a,TRC}}{\dot{Q}_{gh,CO2,TRC}} \tag{9}$$

Power-to-power efficiency (*P2P*) is introduced to evaluate RTCCB's comprehensive performance:

$$P2P = COP \times \eta_{TRC} \tag{10}$$

Note that the *P2P* value corresponds to the same η_{IHX} in both modes. Therefore, the performance comparison indicators between the system with and without a recuperator are listed in Table 1, where *X* can denote the optimal *COP*, η_{TRC}, and *P2P* within the given ranges (opt. and ltd.), and *OHP* is the optimum high pressure.

Table 1: Performance comparison indicators between IHX and basic systems (He *et al.*, 2023)

Items	IHX vs Basic at opt. range	IHX vs Basic at ltd. range
ΔX	$\Delta X_{opt} = (X_{IHX,opt} - X_{bas,opt})/X_{bas,opt}$	$\Delta X_{ltd} = (X_{IHX,ltd} - X_{bas,ltd})/X_{bas,ltd}$
ΔOHP	$\Delta OHP_{opt} = OHP_{IHX,opt} - OHP_{bas,opt}$	$\Delta OHP_{ltd} = OHP_{IHX,ltd} - OHP_{bas,ltd}$
$\Delta T_{cmp,ex}$	$\Delta T_{cmp,ex,opt} = T_{dis,IHX,opt} - T_{dis,bas,opt}$	$\Delta T_{cmp,ex,ltd} = T_{dis,IHX,ltd} - T_{dis,bas,ltd}$

3.2 Validation

The model outputs of this study are compared with the simulation results of basic cycles by Baik *et al.* (2014), with the same $\dot{m}_{CO2}$, high pressure, machine efficiency, pinch points, and secondary fluid temperature of heat exchangers. In the THP mode, the error of the $T_{cmp,ex}$ is below 2 K, and the deviations of compressor power and heat transfer rates of HPHX/LPHX are less than 3 %, and the error of evaporator inlet quality is within 0.01. In the TRC mode, the error of the $T_{exp,su}$ is below 1.5 K, and the deviations of expander/pump power and heat transfer rates of HPHX/LPHX are less than 4 %. The error of condensation pressure is within 1 bar.

3.3 Parameter Setting

All parameters before the further parameter study are set as shown in Table 2. The maximum efficiency for the compressor/expander here is set at 0.85 (Kim *et al.*, 2008; Li *et al.*, 2023; Zhao *et al.*, 2022), which represents their efficiency when over-compression, under-compression, over-expansion, or under-expansion does not occur. For the scroll compressor, if over-compression occurs, the pressure at the adaptive point is higher than the discharge pressure (Zheng *et al.*, 2020). Therefore, the built-in volume ratio (R_V) is set at 2.0 in this study to prevent severe over-compression. Thus, the operating boundaries in this study are: maximum high pressure ($P_{cmp,ex}$ in THP, $P_{exp,su}$ in the TRC) is 140 bar (Li *et al.*, 2025; Volkswagen, 2021; Zhang *et al.*, 2024), and the highest temperature is 150 °C (Zheng *et al.*, 2020). The pinch points of all heat exchangers in both modes are 2 K, and the efficiency of the secondary fluid pump and air fan is 0.7 (Dumont and Lemort, 2020). The CO_2 pump efficiency is 0.85 (Baik *et al.*, 2014; Morandin *et al.*, 2013). This study focuses on the impact of the introduced recuperator (IHX) and the operational boundaries of the scroll machine on the *COP* and η_{TRC}, so the swept volume of the scroll compressor is set as a unity value (1 cm^3). The swept volume of the expander is 0.5 cm^3, which is the compressor swept volume divided by R_V, according to Lemort *et al.* (2009).

Table 2: Parameter settings in the modelling

Parameter	Value	Parameter	Value
$\eta_{cmp,max}$	0.85	$Pinch_{gc,THP}$	2 K
$\eta_{exp,max}$	0.85	$Pinch_{ev,THP}$	2 K
η_{IHX}	0.75	$Pinch_{gh,TRC}$	2 K
$\eta_{pp,CO2}$	0.85	$Pinch_{cd,TRC}$	2 K
$\Delta T_{OH,THP}$	5 K	$\Delta T_{SC,TRC}$	5 K
$\Delta T_{SC,THP}$	5 K	$P_{scroll,max}$	140 bar
R_V	2	$T_{scroll,max}$	150 °C
$c_{p,oil}$	2100 J/kg/K	ρ_{oil}	800 kg/m^3
$c_{p,a}$	1012 J/kg/K	ρ_a	1.23 kg/m^3
$\eta_{pp,oil}$	0.7	$\eta_{fan,a}$	0.7

4 RESULTS AND DISCUSSIONS

4.1 Optimal operation range

Without the constraints of the scroll machine operation boundaries, the optimal operation points of the THP/TRC can be reached. Figure 2 presents the ΔCOP_{opt}, $\Delta\eta_{opt}$, and $\Delta P2P_{opt}$ of the IHX (η_{IHX} = 0.75) and basic RTCCB system without limits. In all operation conditions, the recuperator can enhance the performance of THP/TRC, with a range of 5.4-16.4 % and 0-10.1 % for ΔCOP_{opt} and $\Delta\eta_{opt}$, respectively. When the $T_{hot,h}$ is 80 °C, the impact of the recuperator on TRC efficiency is negligible, because the expander exhaust temperature is low and thus the heat transfer rate of the recuperator is neglectable compared to that of HPHX/LPHX. For the THP, $T_{hot,l}$ has a stronger impact than $T_{hot,h}$, especially when $T_{hot,l}$ > 55 °C, because it affects the gas cooler exhaust temperature, with which ΔCOP_{opt} varies almost linearly (He *et al.*, 2023). In the TRC mode, $\Delta\eta_{opt}$ is mainly influenced by $T_{hot,h}$ in most of conditions, as the $\eta_{opt,IHX}$ is more sensitive to $T_{hot,h}$ than $\eta_{opt,bas}$ with the same η_{exp} and $\eta_{pp,CO2}$ (Wu *et al.*, 2018), and the increment of $T_{hot,h}$ denotes to higher $\Delta\eta_{opt}$. The $P2P_{opt}$ can be increased by 5.9-28.1 %, and its deviation is more sensitive to $T_{hot,h}$ when $T_{hot,l}$ is low, and more sensitive to $T_{hot,l}$ when it is higher. Figure 3 presents the $\Delta OHP_{opt,THP}$, $\Delta OHP_{opt,TRC}$, and $\Delta T_{cmp,ex,opt}$ in both systems. The recuperator can decrease the OHP_{THP} and OHP_{TRC} in all considered conditions, but the cost is that $T_{cmp,ex}$ is lifted by 34 K. It has no impact on the $T_{exp,su}$ because this is determined by the $T_{hot,h}$ and $Pinch_{gh,TRC}$.

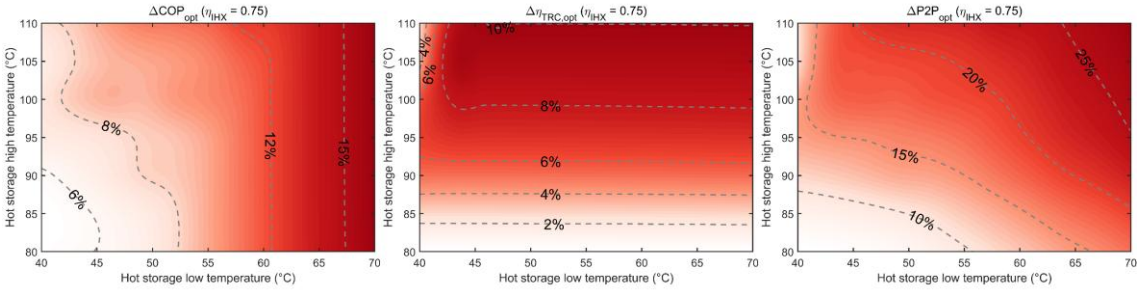

Figure 2: Impact of IHX on ΔCOP_{opt}, $\Delta\eta_{TRC,opt}$, and $\Delta P2P_{opt}$ at optimal operation (η_{IHX} = 0.75)

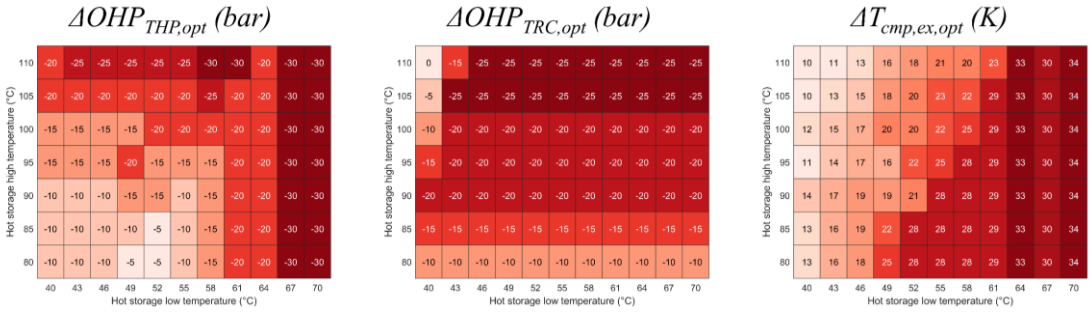

Figure 3: Impact of IHX on $\Delta OHP_{THP,opt}$, $\Delta OHP_{TRC,opt}$, and $\Delta T_{cmp,ex,opt}$ (η_{IHX} = 0.75)

4.2 Limited operation range

When the $P_{scroll,max}$ is 140 bar (Volkswagen, 2021), the operation conditions are limited for the basic system: $T_{hot,h} \leq$ 95 °C, because the minimum pressure in the gas cooler is above 140 bar when the $T_{hot,h}$ is higher. However, the recuperator can extend the possible condition range of the THP, so IHX system can work within 80 ≤ $T_{hot,h}$ ≤ 110 °C. The function of recuperator is only discussed within 80 ≤ $T_{hot,h}$ ≤ 95 °C in this section, which is clarified in Figure 4. The highest compressor discharge pressure is limited in the basic THP, and the optimum high pressure is not reachable (the affected conditions are framed in green dotted lines), so ΔCOP_{ltd} is much higher than ΔCOP_{opt}, thanks to that the $OHP_{ltd,THP}$ is lower when this IHX is adapted. The ability of the recuperator for the decline of optimum high pressure has been discussed in Section 4.1, and it makes more sense in the limited operation. Similarly, in the basic TRC, when $T_{hot,h} \geq$ 85 °C, the OHP_{TRC} is limited to 140 bar (affected conditions are framed in black dotted

lines), and $\Delta\eta_{TRC,ltd}$ is slightly higher than $\Delta\eta_{TRC,opt}$, as its $OHP_{TRC,opt}$ is lower originally (150 bar at $T_{hot,h}$ = 95 °C). As a result, the $\Delta P2P_{ltd}$ has a significant lift compared to $\Delta P2P_{opt}$. Fewer conditions are affected by the operation limits after the introduction of the recuperator in both modes.

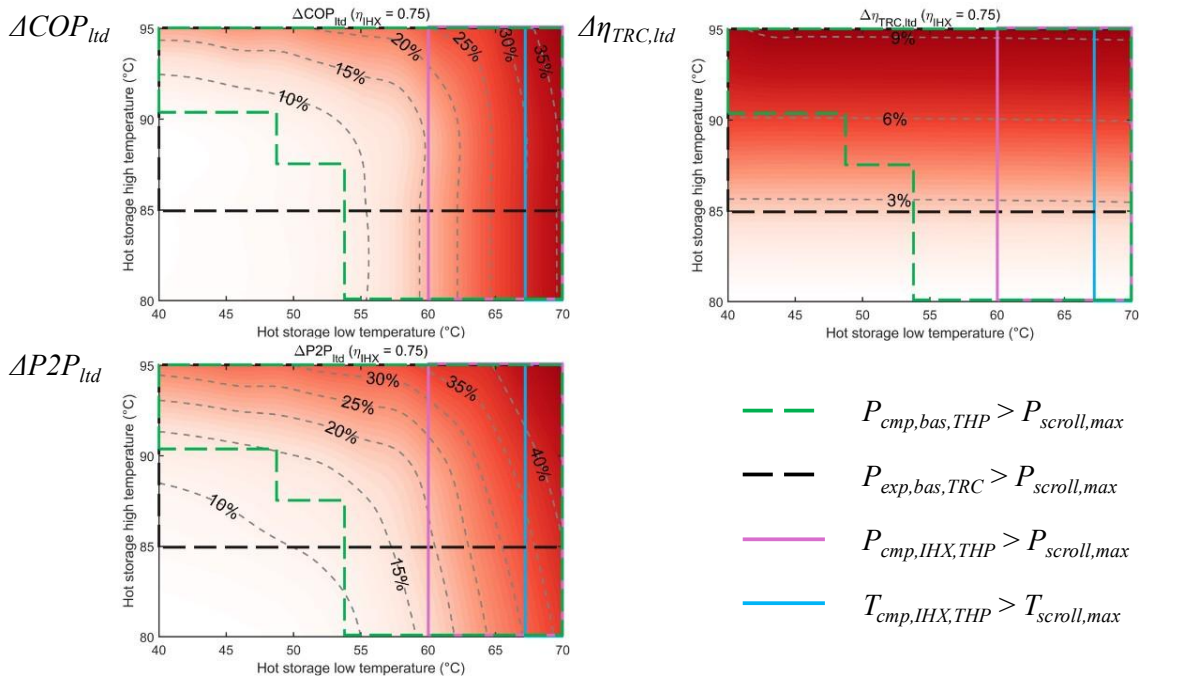

Figure 4: Impact of IHX on ΔCOP_{ltd}, $\Delta\eta_{TRC,ltd}$, and $\Delta P2P_{ltd}$ at limited operation (η_{IHX} = 0.75)

Figure 5 presents the absolute values of the COP_{THP} and η_{TRC} with/without IHX under optimal/limited operation ranges. When $T_{hot,l}$ < 45 °C and $T_{hot,h}$ > 100 °C, $OHP_{TRC,IHX}$ is higher for a better match with the larger ($T_{hot,h}$ - $T_{hot,l}$) in the HPHX, resulting in a drop of $\eta_{TRC,IHX,opt}$ and $\eta_{TRC,IHX,ltd}$.

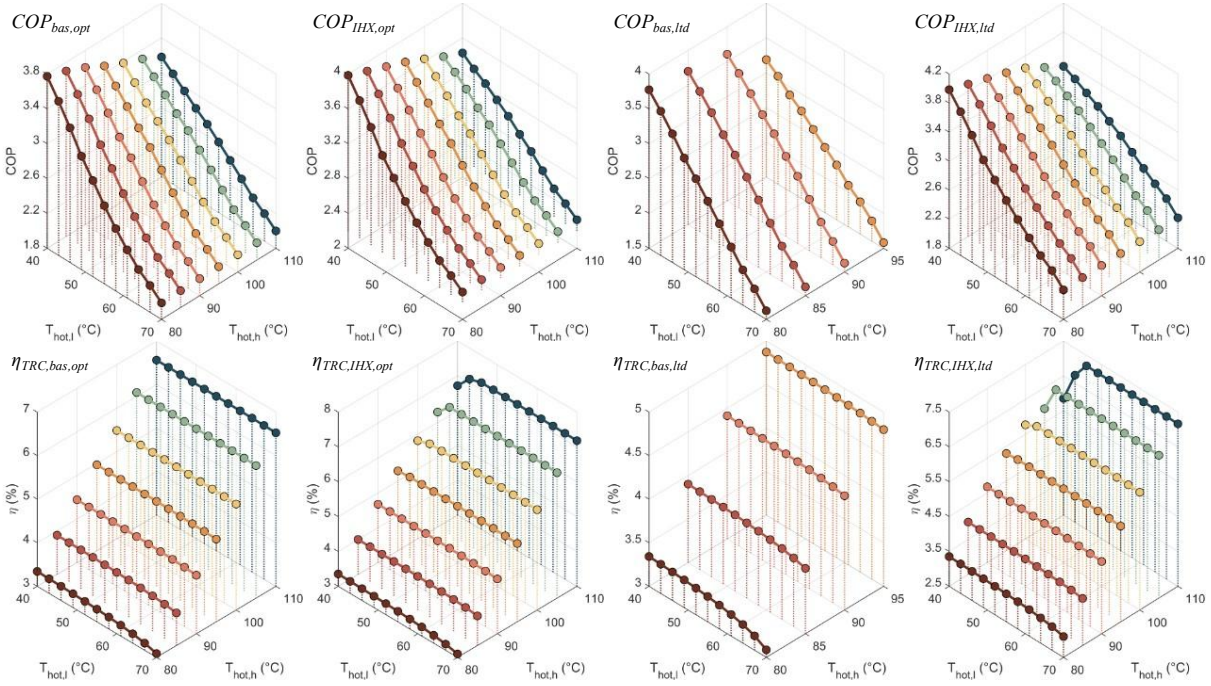

Figure 5: COP_{THP} and η_{TRC} with/without IHX under optimal/limited operation (η_{IHX} = 0.75)

When η_{IHX} is 0.75, the affected region of OHP_{THP} is not eliminated, only narrowing from the green dotted frame to the purple solid frame, but it occurs that the operational high pressure of the THP system with a recuperator deviates from its optimum value due to the highest temperature limit when $T_{hot,l}$ > 67 °C (the affected conditions are framed in blue solid lines). Experimentally, the η_{IHX} can vary within 0.3 – 0.96 under different heat exchange areas (Otón-Martínez *et al.*, 2022), so what will happen with the variation of η_{IHX}? Figure 6 delineates the variation of $\Delta P2P_{ltd}$ with four η_{IHX} values. When η_{IHX} = 0.25, the affected region of OHP_{TRC} narrows from the black dotted frame to the orange solid frame, and it does not exist after η_{IHX} = 0.5. When η_{IHX} is above 0.5, the characteristic of the recuperator that it increases the $T_{cmp,ex}$, starts to introduce a disadvantage that the high pressure of THP is reduced from the OHP_{THP} due to the temperature limit (in blue solid lines), and more conditions are affected with the η_{IHX} from 0.75 to 1. This slows down the increasing rate of $\Delta P2P_{ltd}$ with η_{IHX}, but the impact of IHX is enhanced by its rising efficiency generally. If the η_{IHX} = 1, the $OHP_{THP,ltd}$ is always below 140 bar.

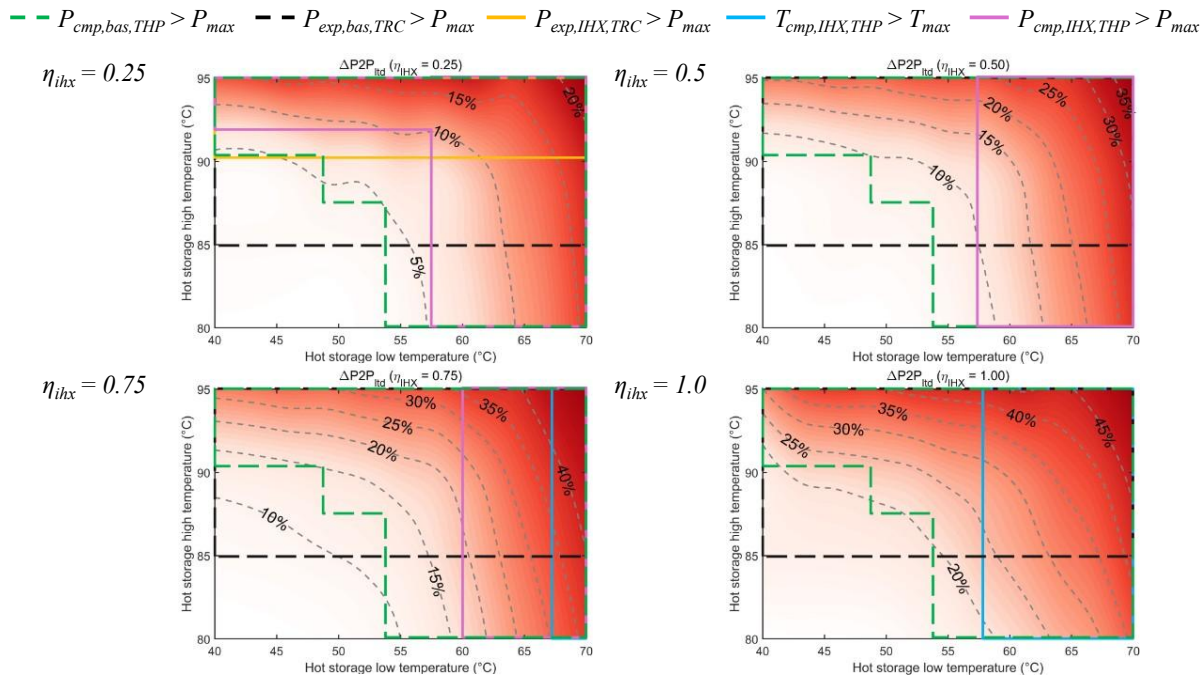

Figure 6: Impact of recuperator efficiency on $\Delta P2P_{ltd}$

4.3 Boundary extension

Practically, the boundaries of a scroll compressor in this study can be extended, and the $P_{scroll,max}$ is enlarged to 160 bar (Jiang *et al.*, 2024), and $T_{scroll,max}$ is increased to 160 °C (Li *et al.*, 2023; Mateu-Royo *et al.*, 2019). Figure 7 shows the ΔCOP_{ltd}, $\Delta\eta_{TRC,ltd}$, and $\Delta P2P_{ltd}$ at $P_{scroll,max}$ = 160 bar and $T_{scroll,max}$ = 150 °C. This enlarges the possible operation range to 80 ≤ $T_{hot,h}$ ≤ 110 °C for the basic system, and there are more unaffected conditions for basic THP/TRC obviously, compared to Figure 4. For the system with a recuperator, the conditions limited by $T_{scroll,max}$ become more, but the limit of $P_{scroll,max}$ does not exist. The improvement effect of the recuperator is weakened because of the large performance lift in the basic THP/TRC with the extension of $P_{scroll,max}$. The $\Delta\eta_{TRC,ltd}$ can reach 10 % when the $T_{hot,h}$ is over 105 °C, although its value within 80 ≤ $T_{hot,h}$ ≤ 95 °C is lower than Figure 4.

Figure 8 presents the performance deviations at $P_{scroll,max}$ = 140 bar and $T_{scroll,max}$ = 160 °C with η_{IHX} = 1, and the discussed conditions are 80 ≤ $T_{hot,h}$ ≤ 95 °C. The extension of $T_{scroll,max}$ does not lessen the affected conditions of basic THP/TRC but reduces slightly those of the THP/TRC with IHX, compared to Figure 6. Hence, the highest $\Delta P2P_{ltd}$ rises from 56.9 % to 67.5 % (η_{IHX} = 1) with the $T_{scroll,max}$ extension. Note that if η_{IHX} = 0.75, there are no affected conditions in both systems due to the limits of the $T_{scroll,max}$ after its extension.

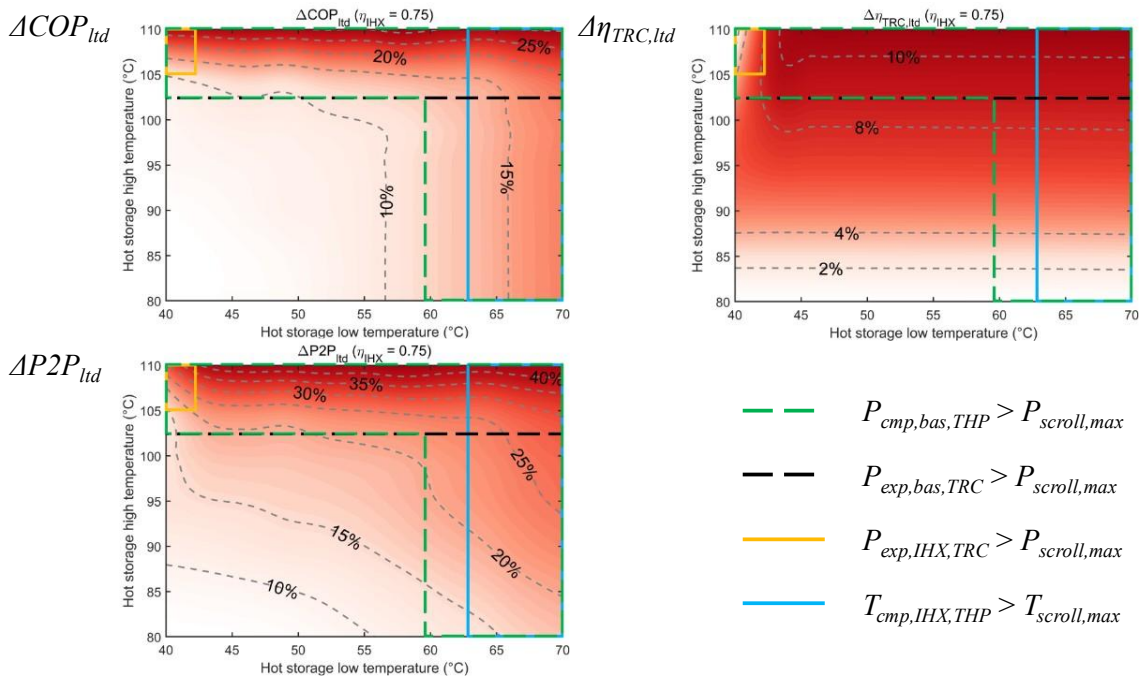

Figure 7: Impact of IHX on ΔCOP_{ltd}, $\Delta\eta_{TRC,ltd}$, and $\Delta P2P_{ltd}$ at $P_{scroll,max}$ = 160 bar (η_{IHX} = 0.75)

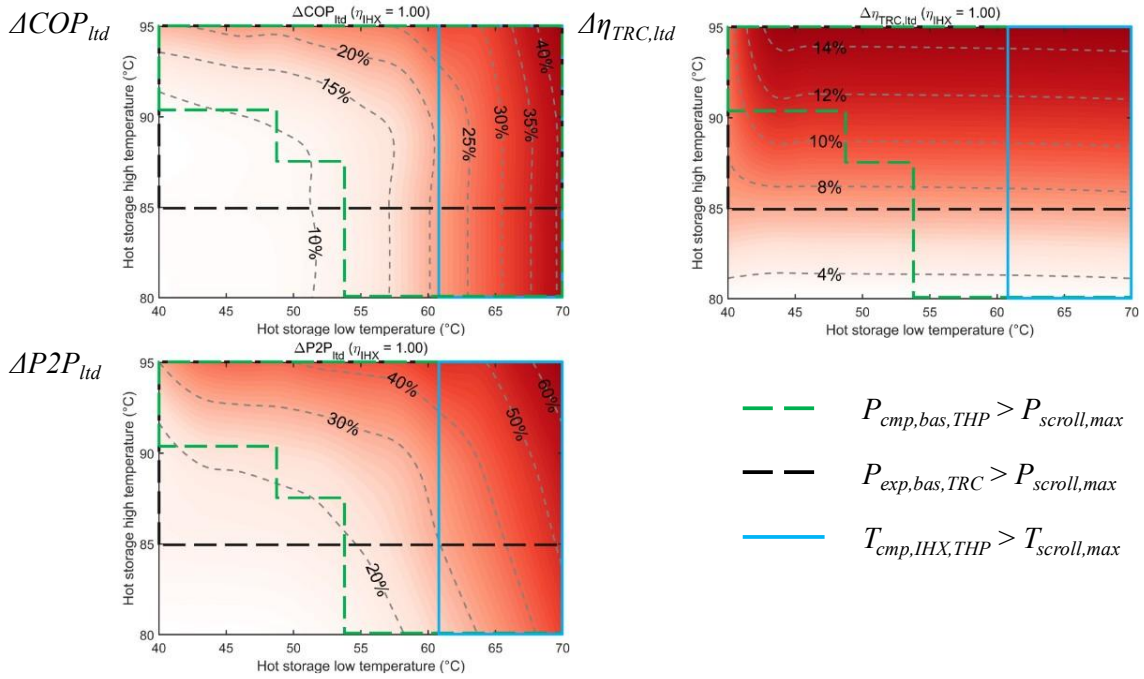

Figure 8: Impact of IHX on ΔCOP_{ltd}, $\Delta\eta_{TRC,ltd}$, and $\Delta P2P_{ltd}$ at $T_{scroll,max}$ = 160 °C (η_{IHX} = 1.00)

4.4 Compression/expansion ratio

In the simulation of Zheng *et al.* (2020), the theoretical pressure ratio (ε_{scroll}) is 2.82 for a scroll compressor, and in the experiment of Li *et al.* (2023), the $\varepsilon_{scroll,max}$ can be over 4. Therefore, the limitation of $\varepsilon_{scroll,max}$ is not discussed in this study, because all conditions discussed above are not limited by it if $\varepsilon_{scroll} < 4$. When $\varepsilon_{scroll,max}$ is set as 2.82, the conditions without $P_{scroll,max}$ extension are not affected, and only basic system at $P_{scroll,max}$ = 160 bar can be limited, whose affected conditions have been represented by those of $P_{scroll,max}$ (green dotted lines in Figure 7).

5 CONCLUSIONS

In this study, the ambient air in the day/night is used as the evaporator/condenser secondary fluid of a reversible CO_2 THP/TRC, respectively. The work focuses on the technical feasibility of a recuperator applied to the reversible trans-critical CO_2 Carnot battery (RTCCB), a scroll compressor acting as the dual-function machine, and the operation boundaries of the scroll machine are considered as operation constraints of the trans-critical HP/Rankine cycle. The main conclusions are as follows:

- In optimal operation without constraints, the recuperator can improve the *COP* of the THP and thermal efficiency of the TRC, decreasing their optimum high pressure, but it increases the discharge temperature of the compressor. If recuperator efficiency is 0.75, ΔCOP_{opt}, $\Delta\eta_{TRC,opt}$, and $\Delta P2P_{opt}$ can be up to 16.4 %, 10.1 %, and 28.1 %, with $\Delta OHP_{opt,THP}$, $\Delta OHP_{opt,TRC}$, and $\Delta T_{cmp,ex,opt}$ reaching -30 bar, -25 bar, and 34 K, respectively.
- In the limited operation of $P_{scroll,max}$ = 140 bar, and $T_{scroll,max}$ = 150 ℃, the affected conditions of the basic THP/TRC are numerous, which can be narrowed by the recuperator. The improvement impact of the recuperator is enlarged in the THP mode compared to the optimal range, and $\Delta P2P_{ltd}$ = 6-53 % with η_{IHX} = 0.75, bringing a higher lift of $\Delta T_{cmp,ex,ltd}$ = 44 K.
- With the recuperator efficiency rising from 0.25 to 1, the conditions that deviate from the optimum pressure due to the $P_{scroll,max}$ limit are fewer, but those deviating from the optimum pressure due to the $T_{scroll,max}$ limit appear from η_{IHX} = 0.75.
- If the $P_{scroll,max}$ is extended to 160 bar, the possible hot storage temperature rises in the system without a recuperator. The affected conditions in the basic THP/TRC are reduced evidently, making ΔCOP_{ltd} and $\Delta P2P_{ltd}$ decrease. If $T_{scroll,max}$ = 160 ℃, its affected conditions in the system with a recuperator are less, and $\Delta P2P_{ltd}$ reaches up to 67.5 % with η_{IHX} = 1.

This work is intended to give recommendations for the design of RTCCB based on Rankine cycle, in choosing operational conditions and scroll machines. The design of the hot storage temperatures and the recuperator size should consider the operation boundaries of the compressor/expander. In future work, the techno-economic feasibility assessment of a recuperator in RTCCB should be conducted, not only for the single-storage configuration in Figure 1, but also for that with cold storage (for instance, ice storage) and hot storage. Additionally, this assessment is based on R_V = 2 for the considered scroll machine, and a more feasible value should be chosen from parametric optimization in the next step. Moreover, a more detailed model should be built, using the same recuperator size instead of the same efficiency in two modes (THP/TRC), to get a more accurate evaluation.

NOMENCLATURE

COP	Coefficient of Performance	(-)	Pinch	pinch point	(K)
c_p	specific heat	(J/kg/K)	$\dot{Q}$	heat transfer rate	(W)
h	enthalpy	(J/kg)	R_V	built-in volume ratio	(-)
$\dot{m}$	mass flow rate	(kg/s)	T	temperature	(℃)
OHP	optimum high pressure	(bar)	$\dot{W}$	power	(W)
P2P	power-to-power efficiency	(-)	ΔT	temperature difference	(K)
P	pressure	(bar)			

Abbreviations

HPHX	high-pressure heat exchanger	TCCB	trans-critical CO_2 Carnot battery
IHX	recuperator (internal heat exchanger)	THP	trans-critical heat pump
LPHX	low-pressure heat exchanger	TRC	trans-critical Rankine cycle
RTCCB	reversible trans-critical CO_2 Carnot battery	TXV	thermal expansion valve

Greek symbols

ε	compression ratio	(-)	ρ	density	(kg/m^3)
η	efficiency	(-)	Δ	deviation	(-)

Subscript

a	air	hot	hot storage
bas	basic system	IHX	recuperator, with a recuperator
cd	condenser	l	low temperature
cmp	compressor	ltd	limited operation
dis	discharge state of compressor	max	maximum
ev	evaporator	oh	overheating
ex	exhaust state	oil	thermal oil
exp	expander	opt	optimal operation
fan	air fan	pp	pump
gc	gas cooler	SC	sub-cooling
gh	gas heater	scroll	scroll machine
h	high temperature		

REFERENCES

Ayachi, F., Ksayer, E. B., Neveu, P., Zoughaib, A., 2016a, Experimental investigation and modeling of a hermetic scroll expander, *Applied Energy*, vol. 181, p. 256-267.

Ayachi, F., Tauveron, N., Tartière, T., Colasson, S., Nguyen, D., 2016b, Thermo-Electric Energy Storage involving CO2 transcritical cycles and ground heat storage, *Applied Thermal Engineering*, vol. 108, p. 1418-1428.

Baik, Y.-J., Heo, J., Koo, J., Kim, M., 2014, The effect of storage temperature on the performance of a thermo-electric energy storage using a transcritical CO2 cycle, *Energy*, vol. 75, p. 204-215.

Bell, I. H., Wronski, J., Quoilin, S., Lemort, V., 2014, Pure and Pseudo-pure Fluid Thermophysical Property Evaluation and the Open-Source Thermophysical Property Library CoolProp, *Industrial & Engineering Chemistry Research*, vol. 53, 6: p. 2498-2508. 10.1021/ie4033999

Caralis, G., Christakopoulos, T., Karellas, S., Gao, Z., 2019, Analysis of energy storage systems to exploit wind energy curtailment in Crete, *Renewable and Sustainable Energy Reviews*, vol. 103, p. 122-139.

Dickes, R., Casati, E., Desideri, A., Lemort, V., Quoilin, S., 2025, Solar-powered organic Rankine cycles: A technical and historical review, *Renewable and Sustainable Energy Reviews*, vol. 212, p. 115319.

Dumont, O., Parthoens, A., Dickes, R., Lemort, V., 2018, Experimental investigation and optimal performance assessment of four volumetric expanders (scroll, screw, piston and roots) tested in a small-scale organic Rankine cycle system, *Energy*, vol. 165, p. 1119-1127.

Dumont, O., Frate, G. F., Pillai, A., Lecompte, S., Lemort, V., 2020, Carnot battery technology: A state-of-the-art review, *Journal of Energy Storage*, vol. 32, p. 101756.

Dumont, O., Lemort, V., 2020, Modelling of a thermally integrated Carnot battery using a reversible heat pump/organic Rankine cycle, *ECOS 2020*,

Dumont, O., Charalampidis, A., Lemort, V., 2021, Experimental investigation of a thermally integrated Carnot battery using a reversible heat pump/organic Rankine cycle, *International Refrigeration and Air Conditioning Conference*, Purdue University: p. 2085

Guo, B., Lemort, V., DESIGNING OF AN OFF-GRID REVERSIBLE HEAT PUMP/ORGANIC RANKINE CYCLE SYSTEM FOR ELECTRICITY AND COOLING DEMANDS OF A NIGERIAN FAMILY FARM, *37th International Conference on Efficiency, Cost, Optimization, Simulation and Environmental Impact of Energy Systems*, ECOS2024: p. 430-441

Guo, B., Lemort, V., Cendoya, A., 2025, Control Strategy and Techno-economic Optimization of a Small-scale Hybrid Energy Storage System: Reversible HP/ORC-based Carnot Battery and Electrical Battery, *Energy*, vol. 329, p. 136508.

He, Y.-J., Tai, Y.-D., Fakrouche, N., Zhang, C.-L., 2023, Applicability evaluation of internal heat exchanger in CO2 transcritical cycle considering compressor operation boundaries, *Applied Energy*, vol. 349, p. 121579.

Jiang, Z., Tian, Y., Li, K., Zhao, Z., Liu, N., Zhang, H., 2024, Research on refrigerant charge determination under different compressor speed and its effects on the performance of transcritical CO2 air-conditioning heat pump system in electric vehicle, *Energy*, vol. 296, p. 131192. https://doi.org/10.1016/j.energy.2024.131192
Kim, H. J., Ahn, J. M., Cho, S. O., Cho, K. R., 2008, Numerical simulation on scroll expander–compressor unit for CO2 trans-critical cycles, *Applied Thermal Engineering*, vol. 28, 13: p. 1654-1661. https://doi.org/10.1016/j.applthermaleng.2007.11.002
Kim, Y.-M., Shin, D.-G., Lee, S.-Y., Favrat, D., 2013, Isothermal transcritical CO2 cycles with TES (thermal energy storage) for electricity storage, *Energy*, vol. 49, p. 484-501.
Lemort, V., 2008, Contribution to the characterization of scroll machines in compressor and expander modes, *University of Liège*, vol. p.
Lemort, V., Quoilin, S., Cuevas, C., Lebrun, J., 2009, Testing and modeling a scroll expander integrated into an Organic Rankine Cycle, *Applied Thermal Engineering*, vol. 29, 14: p. 3094-3102. https://doi.org/10.1016/j.applthermaleng.2009.04.013
Li, G., Ma, J., Zou, H., Zhang, R., 2023, Experimental investigation of refrigerant charge determination for heating performance in a CO2 heat pump system for electric vehicles, *Applied Thermal Engineering*, vol. 233, p. 121147. https://doi.org/10.1016/j.applthermaleng.2023.121147
Li, J., Wang, W., Song, Y., Yang, X., Cao, F., 2025, Adaptive fuzzy PI control for the dynamic operation of the transcritical CO2 thermal system in electric vehicles, *Applied Thermal Engineering*, vol. 259, p. 124737. https://doi.org/10.1016/j.applthermaleng.2024.124737
Mateu-Royo, C., Navarro-Esbrí, J., Mota-Babiloni, A., Molés, F., Amat-Albuixech, M., 2019, Experimental exergy and energy analysis of a novel high-temperature heat pump with scroll compressor for waste heat recovery, *Applied Energy*, vol. 253, p. 113504. https://doi.org/10.1016/j.apenergy.2019.113504
Morandin, M., Mercangöz, M., Hemrle, J., Maréchal, F., Favrat, D., 2013, Thermoeconomic design optimization of a thermo-electric energy storage system based on transcritical CO2 cycles, *Energy*, vol. 58, p. 571-587. https://doi.org/10.1016/j.energy.2013.05.038
Otón-Martínez, R. A., Illán-Gómez, F., García-Cascales, J. R., Velasco, F., Haddouche, M. R., 2022, Impact of an internal heat exchanger on a transcritical CO2 heat pump under optimal pressure conditions: Optimal-pressure performance of CO2 heat pump with IHX, *Applied Thermal Engineering*, vol. 215, p. 118991.
Pan, L., Li, B., Wei, X., Li, T., 2016, Experimental investigation on the CO2 transcritical power cycle, *Energy*, vol. 95, p. 247-254.
Pezo, M., Cuevas, C., Wagemann, E., Cendoya, A., 2024, Net zero energy building technologies–Reversible heat Pump/Organic Rankine cycle coupled with solar collectors and combined heat Pump/Photovoltaics–Case study of a Chilean mid-rise residential building, *Applied Thermal Engineering*, vol. p. 123683.
Qin, X., Wang, D., Jin, Z., Wang, J., Zhang, G., Li, H., 2021, A comprehensive investigation on the effect of internal heat exchanger based on a novel evaluation method in the transcritical CO2 heat pump system, *Renewable Energy*, vol. 178, p. 574-586.
Quoilin, S., Lemort, V., Lebrun, J., 2010, Experimental study and modeling of an Organic Rankine Cycle using scroll expander, *Applied energy*, vol. 87, 4: p. 1260-1268.
Ravindran, R. V., Cotter, D., Wilson, C., Huang, M. J., Hewitt, N. J., 2024, Experimental investigation of a small-scale reversible high-temperature heat pump− organic Rankine cycle system for industrial waste heat recovery, *Applied Thermal Engineering*, vol. 257, p. 124237.
Shamsi, S. S. M., Barberis, S., Maccarini, S., Traverso, A., 2024, Large scale energy storage systems based on carbon dioxide thermal cycles: A critical review, *Renewable and Sustainable Energy Reviews*, vol. 192, p. 114245.
Song, Y., Cui, C., Yin, X., Cao, F., 2022, Advanced development and application of transcritical CO2 refrigeration and heat pump technology—A review, *Energy Reports*, vol. 8, p. 7840-7869.
Sorknæs, P., Thellufsen, J. Z., Knobloch, K., Engelbrecht, K., Yuan, M., 2023, Economic potentials of carnot batteries in 100% renewable energy systems, *Energy*, vol. 282, p. 128837.
Volkswagen, 2021, SSP 881213 - Air Conditioning and Heat Pump in MEB Vehicles 2025, March 5: https://vw-us.erwin-store.com/erwin/showArticleProperties.do?articleId=185907

Wang, F., Wu, W., Huang, Y., Zhang, H., Yu, Q., 2023, Experimental study on optimal heating cycle characteristics of CO2 secondary throttling heat pump system for electric vehicles, *Energy Conversion and Management*, vol. 295, p. 117626.
Wang, J., Belusko, M., Evans, M., Liu, M., Zhao, C., Bruno, F., 2022, A comprehensive review and analysis on CO2 heat pump water heaters, *Energy Conversion and Management: X*, vol. 15, p. 100277.
Wieland, C., Schifflechner, C., Braimakis, K., Kaufmann, F., Dawo, F., Karellas, S., Besagni, G., Markides, C. N., 2023, Innovations for organic Rankine cycle power systems: Current trends and future perspectives, *Applied Thermal Engineering*, vol. 225, p. 120201.
Winandy, E., O, C. S., Lebrun, J., 2002, Experimental analysis and simplified modelling of a hermetic scroll refrigeration compressor, *Applied Thermal Engineering*, vol. 22, 2: p. 107-120. https://doi.org/10.1016/S1359-4311(01)00083-7
Wu, C., Wang, S.-s., Li, J., 2018, Parametric study on the effects of a recuperator on the design and off-design performances for a CO2 transcritical power cycle for low temperature geothermal plants, *Applied Thermal Engineering*, vol. 137, p. 644-658. https://doi.org/10.1016/j.applthermaleng.2018.04.029
Zhang, Z., Wang, S., Zhang, P., Guan, Z., Chang, L., Wang, H., 2024, Effect of the refrigerant charge on transcritical CO2 direct evaporation ice-making system, *Applied Thermal Engineering*, vol. 248, p. 123283. https://doi.org/10.1016/j.applthermaleng.2024.123283
Zhao, Y., Song, J., Liu, M., Zhao, Y., Olympios, A. V., Sapin, P., Yan, J., Markides, C. N., 2022, Thermo-economic assessments of pumped-thermal electricity storage systems employing sensible heat storage materials, *Renewable Energy*, vol. 186, p. 431-456.
Zheng, S., Wei, M., Song, P., Hu, C., Tian, R., 2020, Thermodynamics and flow unsteadiness analysis of trans-critical CO2 in a scroll compressor for mobile heat pump air-conditioning system, *Applied Thermal Engineering*, vol. 175, p. 115368.

ACKNOWLEDGEMENT

The authors would like to acknowledge the support of the project "REPTES - Renewable plants integrated with pumped thermal energy storage for sustainable satisfaction of energy and agricultural needs of African communities" under LEAP-RE programme, which has received funding from the European Union's Horizon 2020 Research and Innovation Program under Grant Agreement 963530. This work was also supported by the Fonds de la Recherche Scientifique - FNRS under Grant(s) n° R.8003.23.